Electronic Supplementary Material (ESI)

Acid-Induced Fluorescence Enhancement of Piperazinylphenyl-substituted Nanographene

Hao Zhao,[a] Rafael Muñoz-Mármol,[b,c] Liliia Moshniaha,[d] Qiqi Yang,[e] Mischa Bonn,[e] Xiaomin Liu,[e] Ryota Kabe,[d] Giuseppe Maria Paternò,*[c,f] and Akimitsu Narita*[a,e]

[a.]Organic and Carbon Nanomaterials Unit, Okinawa Institute of Science and Technology Graduate University, 1919-1 Tancha, Onna-son, Kunigami-gun, Okinawa 904-0495, Japan. E-mail: akimitsu.narita@oist.jp

[b.]Instituto Universitario de Materiales, University of Alicante, San Vicente del Raspeig 03690, Spain

[c.]Physics Department, Politecnico di Milano, Piazza L. da Vinci 32, 20133 Milano, Italy. E-mail: giuseppemaria.paterno@polimi.it

[d.]Organic Optoelectronics Unit, Okinawa Institute of Science and Technology Graduate University, 1919-1 Tancha, Onna-son, Kunigami-gun, Okinawa 904-0495, Japan

[e.]Max Planck Institute for Polymer Research Ackermannweg 10, 55128 Mainz, Germany

[f.]Center for Nanoscience and Technology, Istituto Italiano di Tecnologia, Milano 20134, Italy

Table of Contents

1. General Experimental Details

The reactions working with air- and/or moisture-sensitive compounds were carried out under argon atmosphere using standard Schlenk line techniques. 3,11-Dibromo-substituted dibenzo[*hi*,*st*]ovalene (**1**) was synthesized according to our previously reported procedure.[1] Anhydrous toluene was purified by a solvent purification system (GlassContour) prior to use. All other starting materials, solvents and reagents were purchased from commercial suppliers and used as received unless otherwise noted. Thin–layer chromatography (TLC) was done on silica gel coated aluminum sheets with F254 indicator and column chromatography separation was performed with silica gel (particle size 0.063-0.200 mm). Nuclear Magnetic Resonance (NMR) spectra were recorded in chloroform-*d* ($CDCl_3$) using Bruker Avance Neo 400 and 500 MHz NMR spectrometers. Chemical shifts (δ) were expressed in ppm relative to the residual of solvents ($CDCl_3$, ^{1}H: 7.26 ppm, ^{13}C: 77.16 ppm). Coupling constants (*J*) were recorded in Hertz. Abbreviations: s = singlet, d = doublet, t = triplet. Proton signals of DBOV–PZP **3** were assigned based on the previous result reported for 6,14-dimesityl-3,11-bis(4-*t*-butylphenyl)dibenzo[*hi*,*st*]ovalene,[1] with the support of ^{1}H,^{1}H–COSY (correlated spectroscopy), ^{1}H,^{1}H–NOESY (nuclear overhauser enhancement spectroscopy), and ^{1}H,^{13}C–HSQC (heteronuclear single-quantum coherence) experiments. High–resolution matrix–assisted laser desorption/ionization time–of–flight mass spectrometry (HR MALDI–TOF MS) was performed using 7,7,8,8-tetracyanoquinodimethane (TCNQ) as matrix on a Bruker MALDI ultrafleXtreme spectrometer.

UV-vis absorption, excitation, photoluminescence, and excitation emission matrix spectra in different argon-filled organic solvents were recorded on the Horiba Duetta fluorescence and absorbance spectrometer. The excitation spectra were measured for 680 nm emission band with the excitation range of 700–350 nm, exposure time of 200 ms, and a detector accumulation of 3. The exposure time for all steady-state fluorescence spectra measurement was set as 200 ms. The excitation emission matrix spectra were measured for the excitation range of 350–700 nm and emission range of 400–1100 nm with an integration time 100 ms. UV-vis absorption and fluorescence spectra during the titration with acid and base were collected on a UV-vis-NIR spectrophotometer (Shimadzu UV–3600 Plus) and Horiba fluorescence spectrometer (Fluoromax_Plus_C_P) using a 10 mm quartz cell, respectively.

The time-resolved emission spectra and decay profiles were recorded at room temperature in argon-filled solutions using a streak camera system (C14832-110, Hamamatsu Photonics) equipped with a 300 mm spectrograph (SpectraPro, HRS-300-SS, Princeton Instruments). The excitation was provided by a Yb:KGW femtosecond laser (PHAROS, Light Conversion) with the optical parametric amplifier (ORPHEUS, Light Conversion). The laser pulse width and frequency were 165 fs and 25 Hz, respectively. The 380 nm wavelength was used for excitation and integration was made for a range of 582 – 845 nm for all samples.

Absolute photoluminescence quantum yields (PLQY) were measured on an integrating sphere with a photoluminescence measurement unit (Quantaurus–QY, C11347-01, Hamamatsu Photonics) in a nitrogen-filled glovebox. The 380 nm wavelength was used for excitation and integration was made for a range of 580 – 940 nm for all samples.

Transient absorption measurements were performed on liquid samples in a 1 mm quartz cuvette with a handmade pump-probe system,[2] driven by a Ti:Sapphire regenerative amplifier (Libra, Coherent) with 4 W fundamental at 800 nm operating at 2 kHz. The laser output (100 fs) was divided in two beams used to generate the pump and probe: *i*) to generate the pump pulses, the corresponding beam was directed into a non-collinear optical parameter amplifier (NOPA) to generate narrow excitation pulses at 570 nm (70 fs temporal resolution); *ii*) broadband probe

pulses were generated focusing the beam in a sapphire plate to cover the 450 to 750 nm spectral range. The probe polarization was adjusted before the white light generation with a $\lambda/2$ waveplate to magic angle (54.7° between pump and probe polarizations) to prevent rotational dynamics. Then, both beams were focus on the same spot of the sample and the pump-probe time delay was set by a mechanical delay stage spanning a 1 ns range. Finally, the probe was analyzed by means of a dispersive spectrometer.

For single-molecule blinking property measurements, the sample was prepared as follows. The coverslips were sonicated in 1% Micro 90 alkaline cleaning solution for 15 min. Then the coverslips were rinsed three times with Milli-Q water and finally dried with nitrogen flow. Afterward, those coverslips were cleaned by oxygen-plasma cleaner (250 W, 10 min). For sample measured in air, 10 μL of a solution of DBOV-PZP **3** (10^{-12} M) in tetrahydrofuran (THF) was spin-coated on the clean coverslip. For sample measured with HCl, 10 μL of a solution of DBOV-PZP **3** (10^{-12} M in THF, with ~4 eq. of HCl) was spin-coated on the clean coverslip. The coverslip was spun at 2,000 rpm for 60 s. Single-molecule blinking property measurements were performed using a super resolution ground state depletion (SR GSD) microscope (Leica). The 488-nm (300 mW) laser was selected for fluorescence reactivation. For the 488-nm laser, the excitation filter (483 nm - 493 nm/400 nm - 410 nm), the dichroic beam splitter (496 nm) and the emission filter (505 nm - 605 nm/449 nm – 451 nm) were used. The objective lens HCX PL APO 160x 1.43 NA Oil CORR-TIRF was selected. The microscope was equipped with an EMCCD camera (iXonDU-897, Andor). The camera settings were 10 MHz at 14 bit and a pre-amplification of 5.1. The camera exposure time was set to 30 ms and an EM gain of 100 was used. Single-molecule fluorescence time trace, photon number per switching event, mean blinking time and the on-off duty cycle were processed and calculated as in our previous report.[3]

2. Synthetic Details

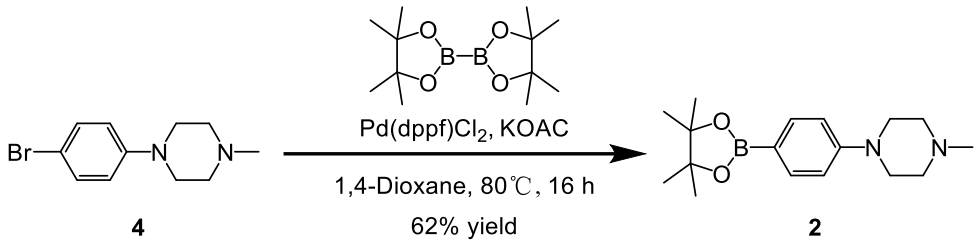

Scheme S1. Synthesis of piperazinylphenyl (PZP)-boronic ester **2**.

1-methyl-4-[4-(4,4,5,5-tetramethyl-1,3,2-dioxaborolan-2-yl)phenyl]piperazine (PZP-boronic ester **2**)

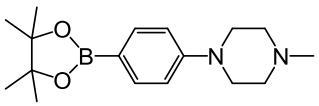

To a Schlenk tube equipped with a stirring bar was added 1-(4-bromophenyl)-4-methylpiperazine (**4**) (500 mg, 1.95 mmol), bis(pinacolato)diboron (990 mg, 3.90 mmol), $Pd(dppf)Cl_2$ (142.7 mg, 0.195 mmol) and potassium acetate (575 mg, 5.85 mmol). The reaction tube was evacuated and backfilled with argon for three times before the addition of anhydrous 1,4-dioxane (20 mL). The mixture was degassed by bubbling with argon for 30 min and heated at 80 ℃ for 16 h. After cooling down to room temperature, water was added and the mixture was extracted with ethyl acetate three times. The organic phases were combined, washed with brine, dried over $MgSO_4$ and evaporated. The residue was purified by silica gel column chromatography (eluent: dichloromethane/methanol = 10/1 v/v) to afford the title compound (367 mg, 62% yield) as brown solid. ^{1}H NMR (400 MHz, $CDCl_3$, 298 K) δ (ppm) 7.71 (d, J = 8.8 Hz, 2H), 6.89 (d, J = 8.8 Hz, 2H), 3.36 – 3.28 (m, 4H), 2.67 – 2.58 (m, 4H), 2.39 (s, 3H), 1.32 (s, 12H). ^{13}C NMR (100 MHz, $CDCl_3$, 298 K) δ (ppm) 153.22, 136.28, 114.59, 83.52, 54.90, 47.97, 46.04, 24.97. HRMS (MALDI, positive): m/z Calcd. for $C_{17}H_{27}BN_2O_2^+$ $[M]^+$: 302.2163; found: 302.2154 (error = –4.0 ppm).

6,14-dimesityl-3,11-bis[4-(4-methylpiperazin-1-yl)phenyl]dibenzo[*hi*,*st*]ovalene (DBOV–PZP **3**)

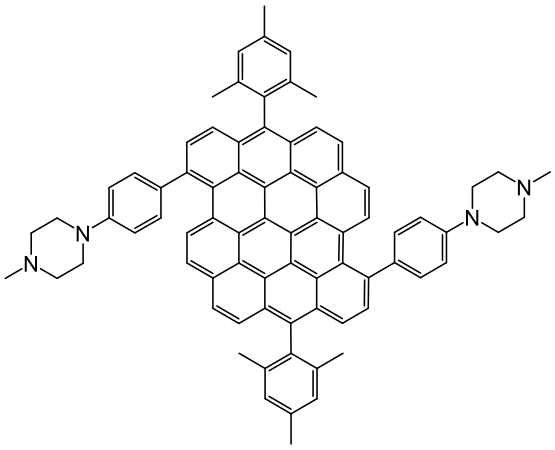

To a Schlenk tube equipped with a stirring bar was added 3,11-dibromo-substituted dibenzo[*hi*,*st*]ovalene **1** (17.4 mg, 20 μmol), PZP-boronic ester **2** (24.2 mg, 80 μmol), $Pd(PPh_3)_4$ (2.3 mg, 2 μmol) and potassium carbonate (27.5 mg, 200 μmol). The reaction tube was evacuated and backfilled with argon three times before the addition of a mixture of toluene/water = 4 mL/1 mL. The mixture was degassed by bubbling with argon for 30 min and heated at 90 °C for 24 h. After cooling down to room temperature, water was added and the mixture was extracted with ethyl acetate for three times. The organic phases were combined, washed with brine, dried over $MgSO_4$ and evaporated. The residue was purified by silica gel column chromatography (eluent: tetrahydrofuran/methanol = 20/1 v/v) to afford the title compound (5.1 mg, 24% yield) as blue solid. ^{1}H NMR (400 MHz, $CDCl_3$, 298 K) δ (ppm) 8.90 (d, J = 8.4 Hz, 2H), 8.07 (d, J = 8.5 Hz, 2H), 7.97 (d, J = 9.2 Hz, 2H), 7.90 (d, J = 8.5 Hz, 2H), 7.86 (d, J = 8.5 Hz, 2H), 7.72 (d, J = 9.2 Hz, 2H), 7.63 (d, J = 8.6 Hz, 4H), 7.23 (s, 4H), 7.09 (d, J = 8.6 Hz, 4H), 3.42 (s, 8H), 2.77 (s, 8H), 2.54 (s, 6H), 2.49 (s, 6H), 1.96 (s, 12H). ^{13}C NMR (125 MHz, $CDCl_3$, 298 K) δ (ppm) 150.41, 138.13, 137.91, 137.53, 137.00, 135.18, 134.80, 132.07, 130.39, 129.92, 129.67, 129.41, 129.30, 128.70, 128.53, 126.67, 126.15, 125.88, 124.74, 123.99, 123.66, 123.00, 122.88, 117.40, 68.13, 55.18, 48.84, 46.18, 25.74, 20.44. HRMS (MALDI, positive): *m*/*z* Calcd. for $C_{78}H_{64}N_4^+$ $[M]^+$: 1056.5131; found: 1056.5109 (error = –2.1 ppm).

3. NMR and HR MALDI–TOF MS Spectra

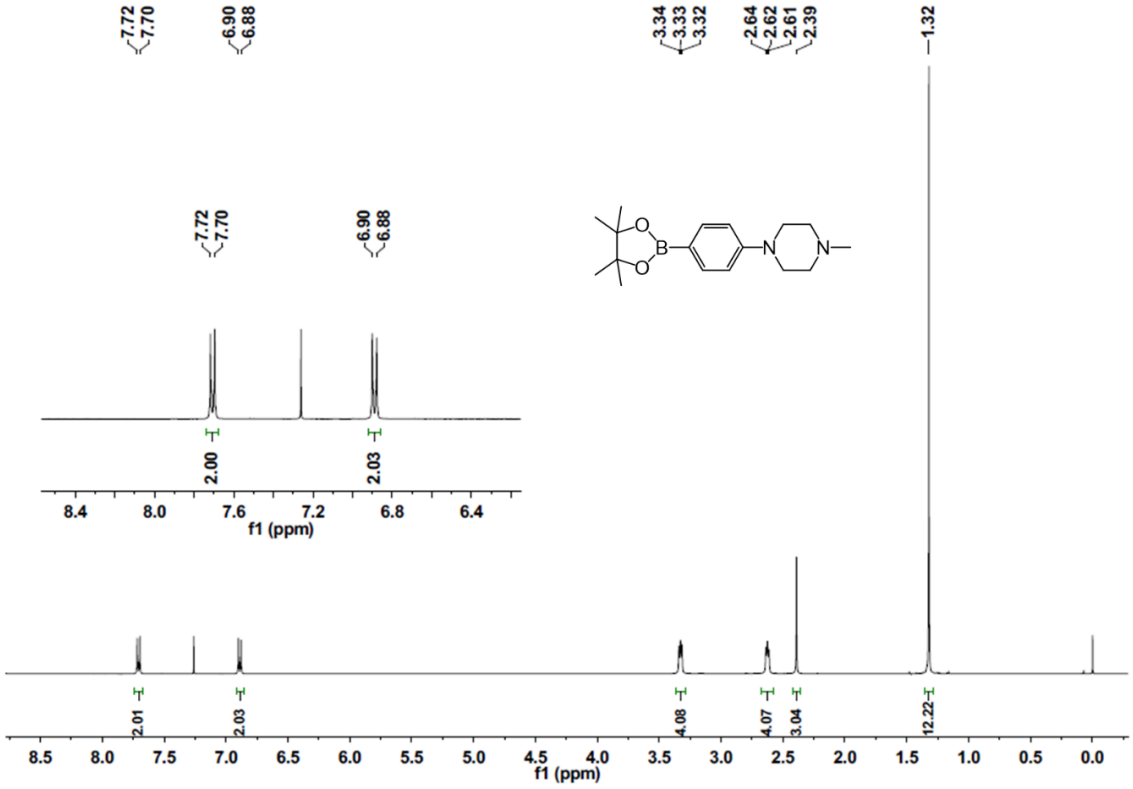

Figure S1. ^{1}H NMR spectrum of compound **2** in $CDCl_3$ (400 MHz, 298 K).

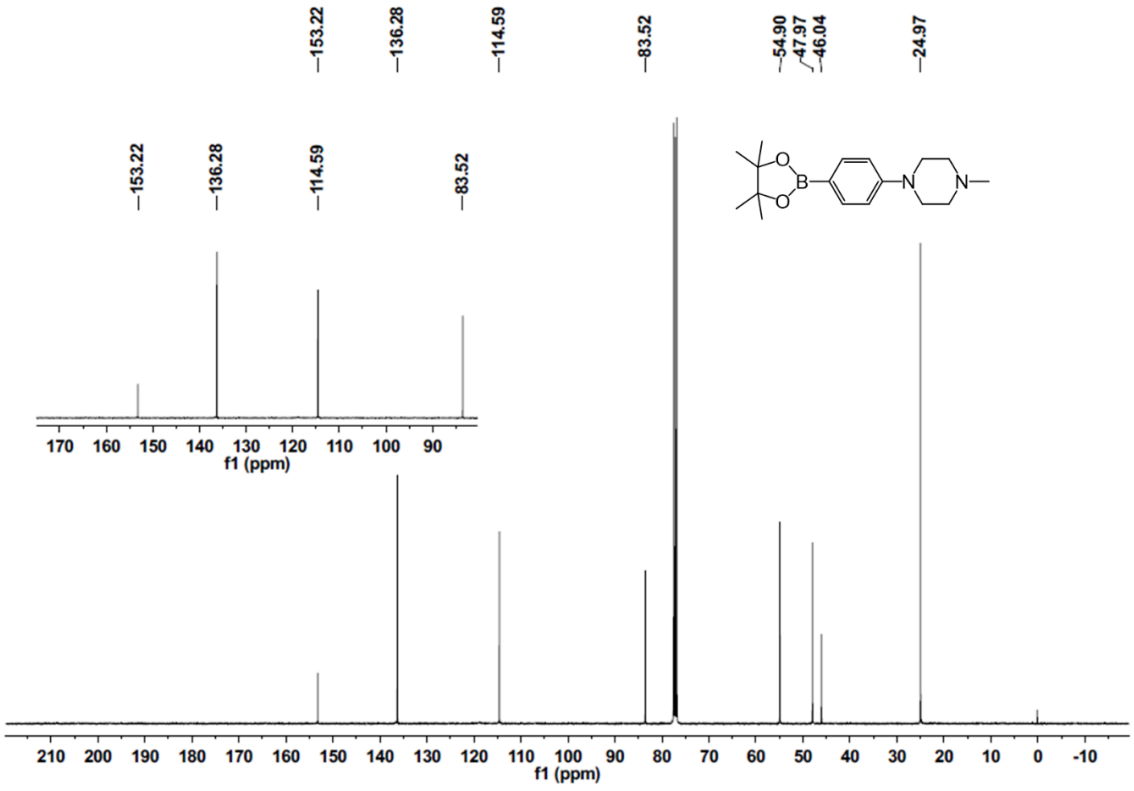

Figure S2. ^{13}C NMR spectrum of compound **2** in $CDCl_3$ (100 MHz, 298 K).

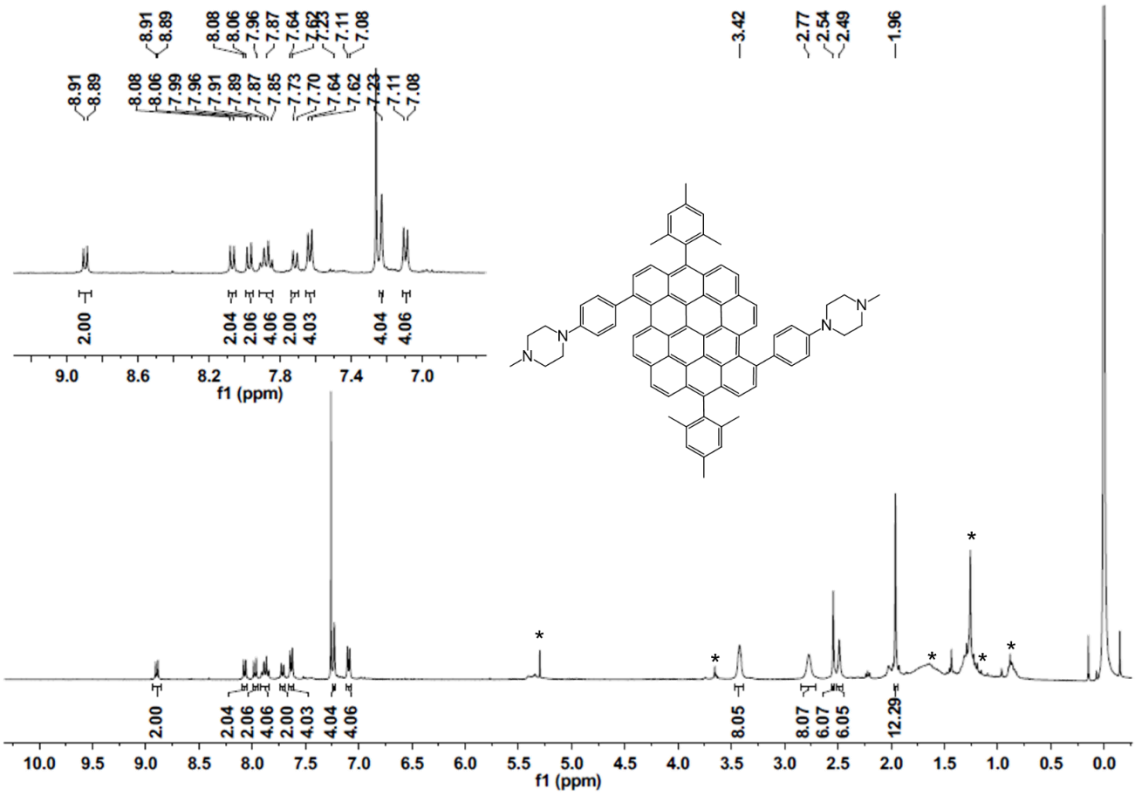

Figure S3. ^{1}H NMR spectrum of compound **3** in $CDCl_3$ (500 MHz, 298 K). *Residual solvent peaks from DCM (dichloromethane), ethanol contained in $CDCl_3$ as the stabilizer, water, and hexane.

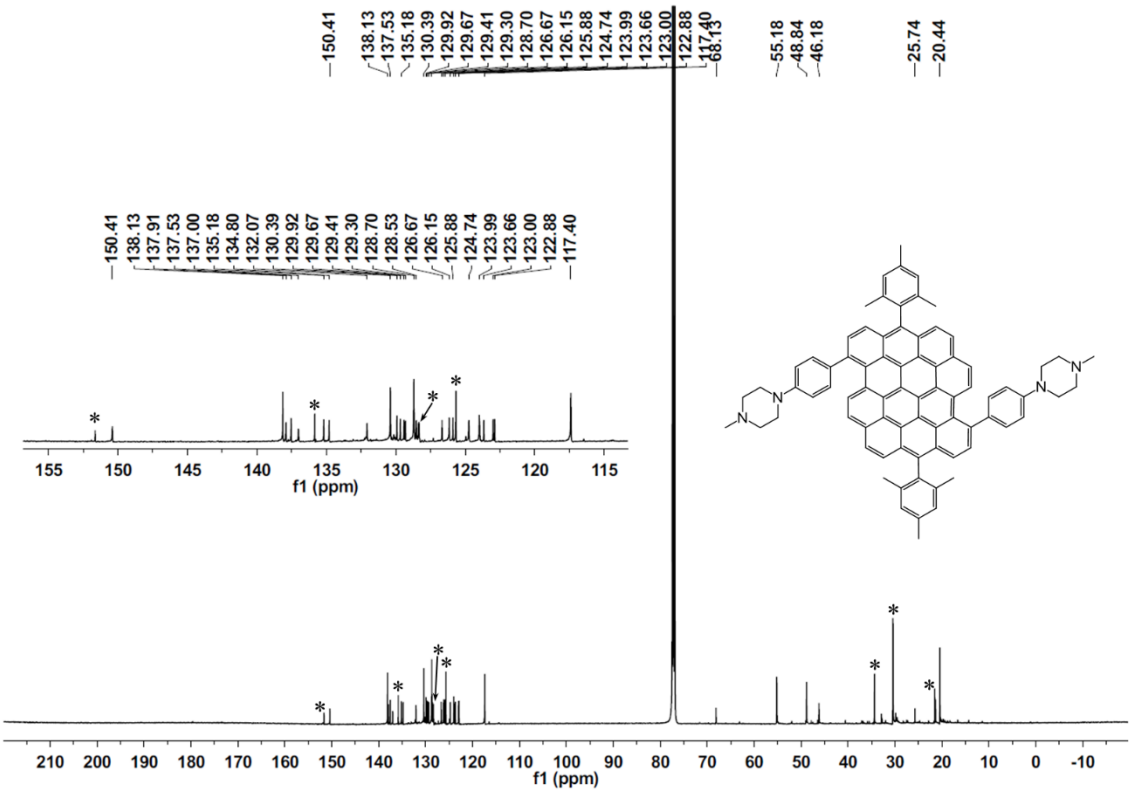

Figure S4. ^{13}C NMR spectrum of compound **3** in $CDCl_3$ (125 MHz, 298 K). *Impurity peaks from BHT (butylate hydroxytoluene) contained in THF as stabilizer.

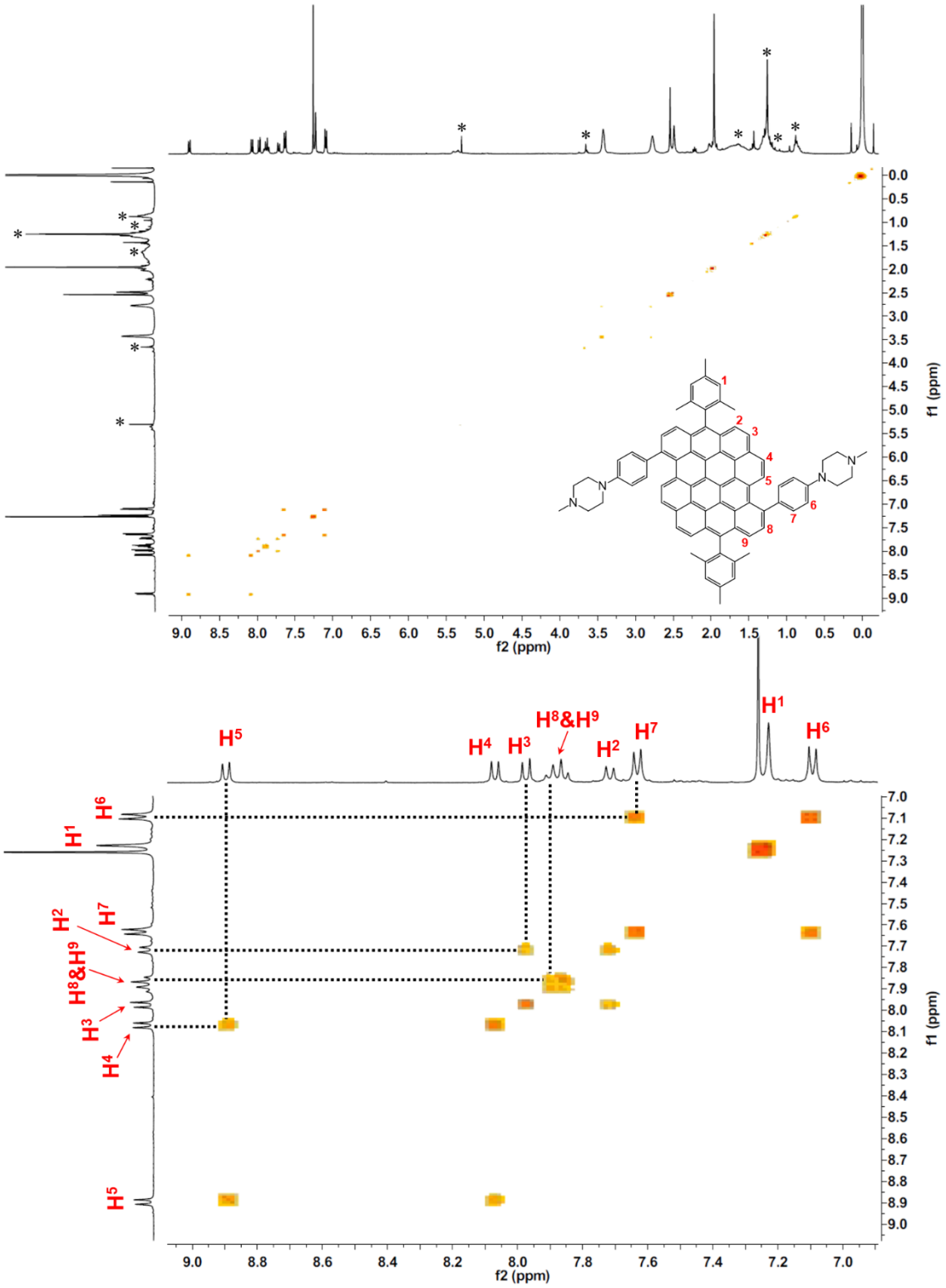

Figure S5. Aromatic region of ^{1}H, ^{1}H–COSY spectrum of compound **3** in $CDCl_3$ (400 MHz, 298 K). *Residual solvent peaks from DCM, ethanol contained in $CDCl_3$ as the stabilizer, water, and hexane.

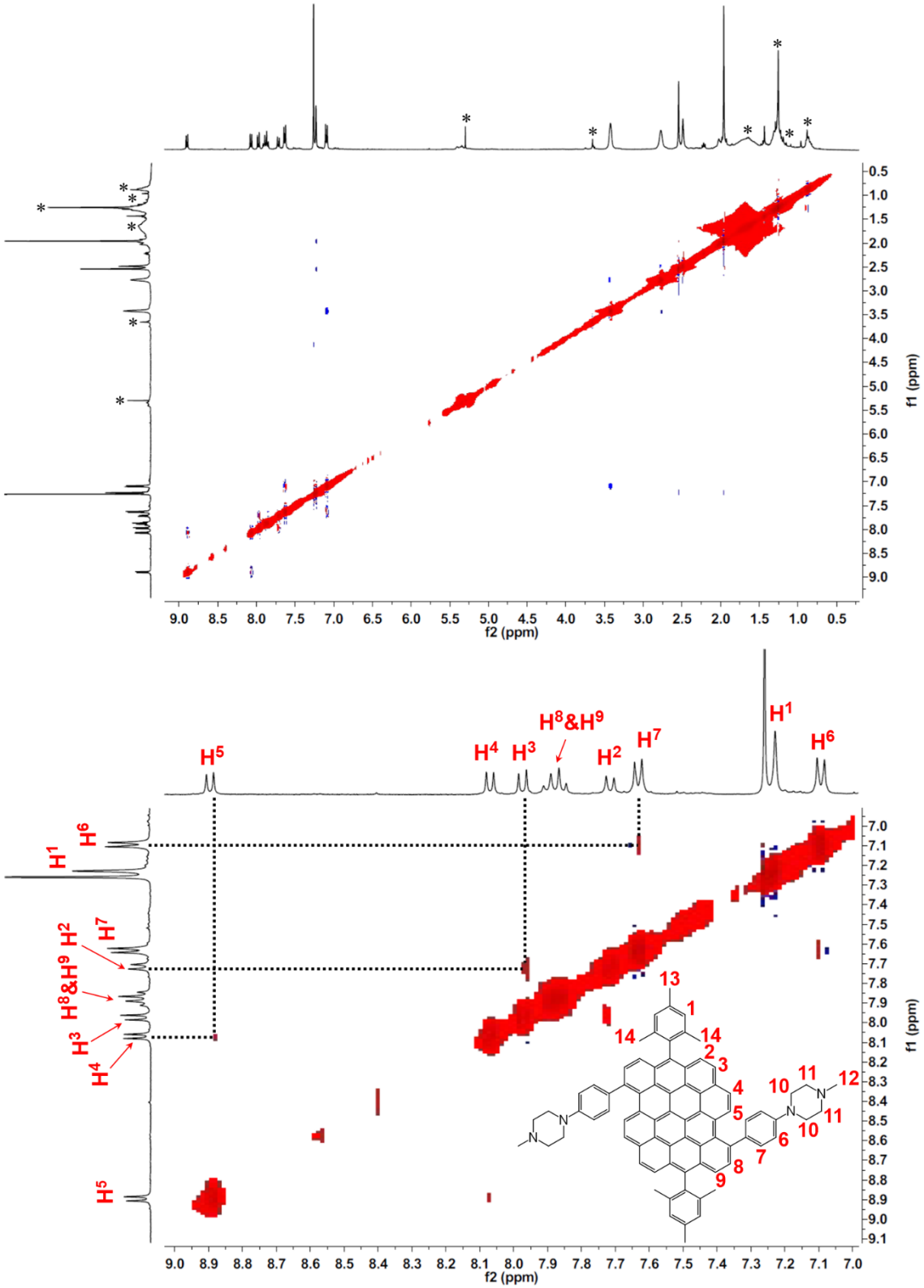

Figure S6. Aromatic region of ^{1}H, ^{1}H–NOESY spectrum of compound **3** in $CDCl_3$ (400 MHz, 298 K). *Residual solvent peaks from DCM, ethanol contained in $CDCl_3$ as the stabilizer, water, and hexane.

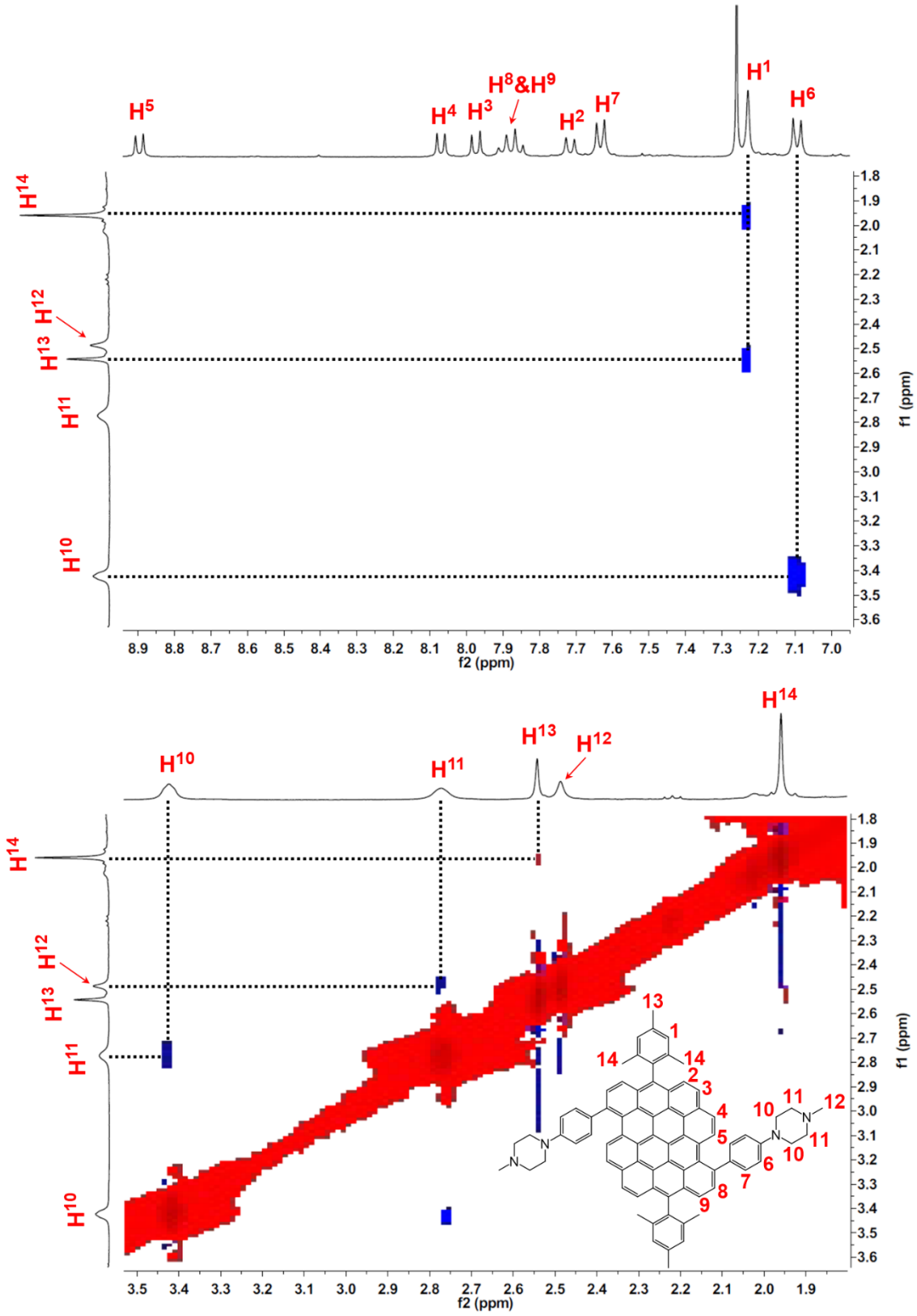

Figure S7. Aliphatic region of ^{1}H, ^{1}H–NOESY spectrum of compound **3** in $CDCl_3$ (400 MHz, 298 K).

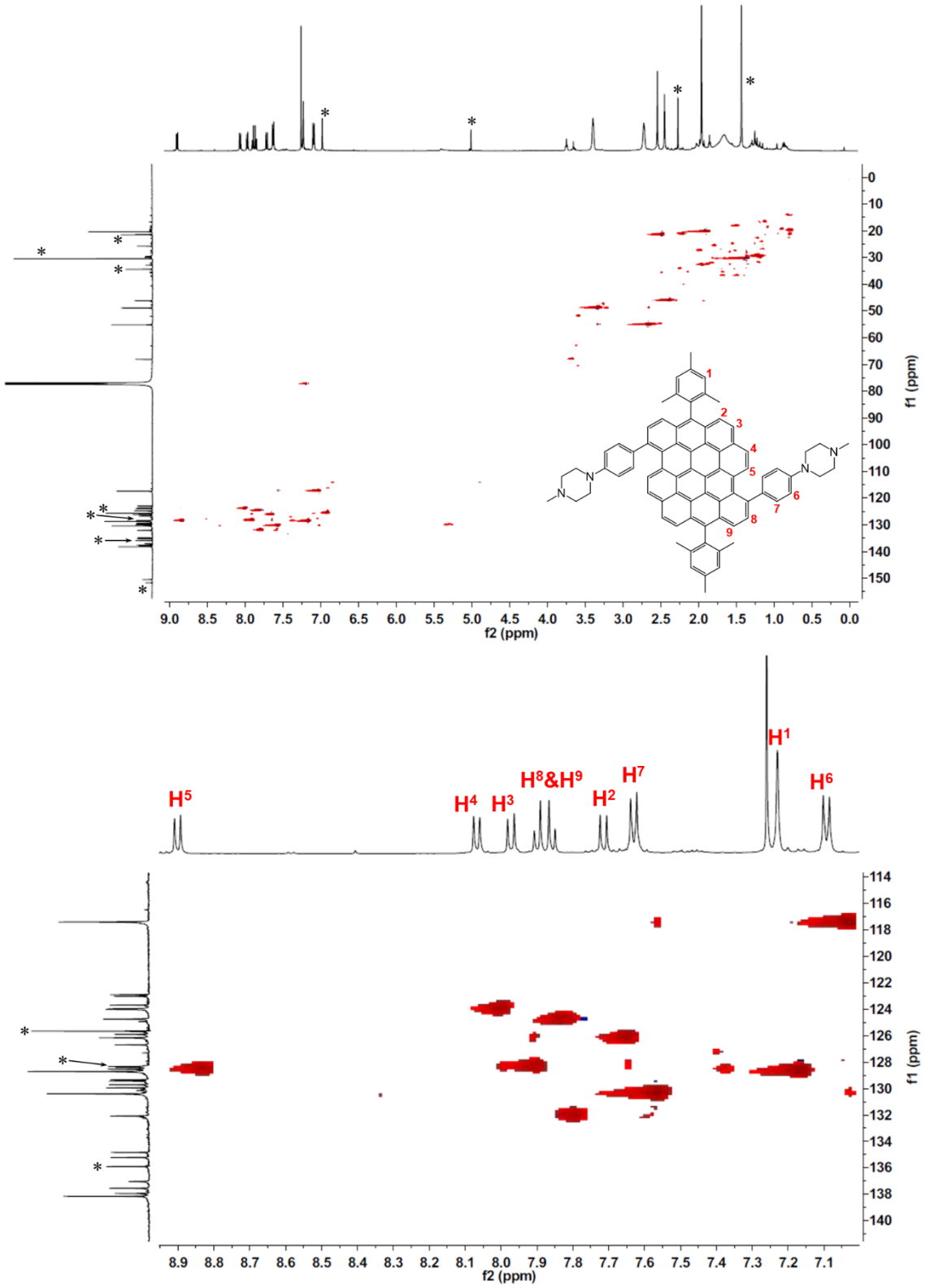

Figure S8. ^{1}H, ^{13}C–HSQC spectrum of compound **3** in $CDCl_3$ (500 MHz, 298 K). *Impurity peaks from BHT contained in THF as stabilizer.

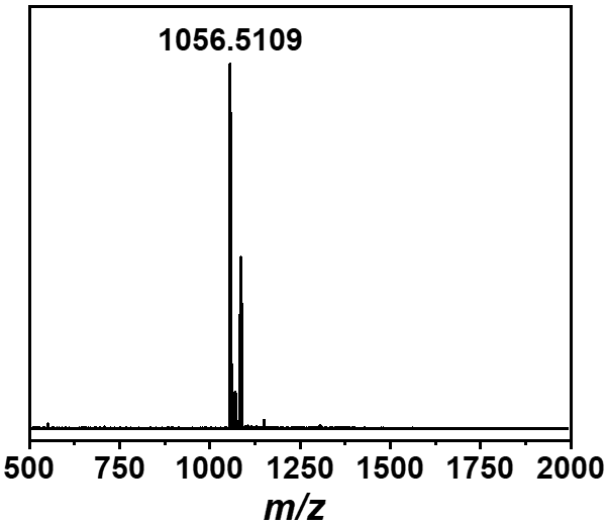

Figure S9. HR MALDI-TOF MS spectrum of DBOV-PZP **3**.

4. UV-Vis Absorption, Excitation, and Fluorescence Spectra of DBOV–PZP 3

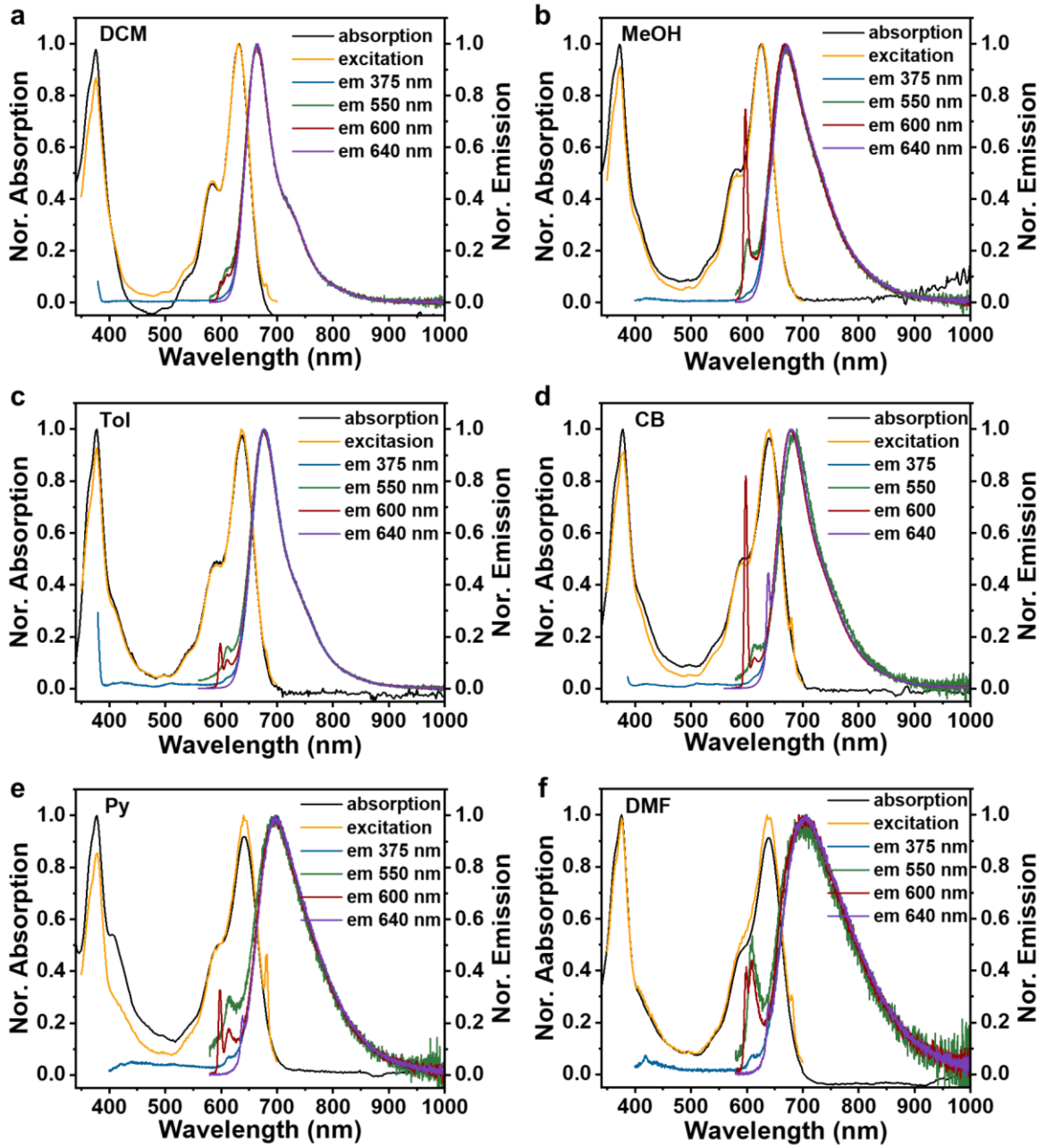

Figure S10. Normalized UV-vis absorption (black), excitation (yellow), and fluorescence spectra measured with different excitation wavelengths (blue – 375 nm, green – 550 nm, red – 600 nm, violet – 640 nm) of DBOV–PZP **3** (2.5×10^{-6} M) in argon-filled (a) dichloromethane (DCM), (b) methanol (MeOH), (c) toluene (Tol), (d) chlorobenzene (CB), (e) pyridine (Py), (f) *N*,*N*-dimethylformamide (DMF), respectively.

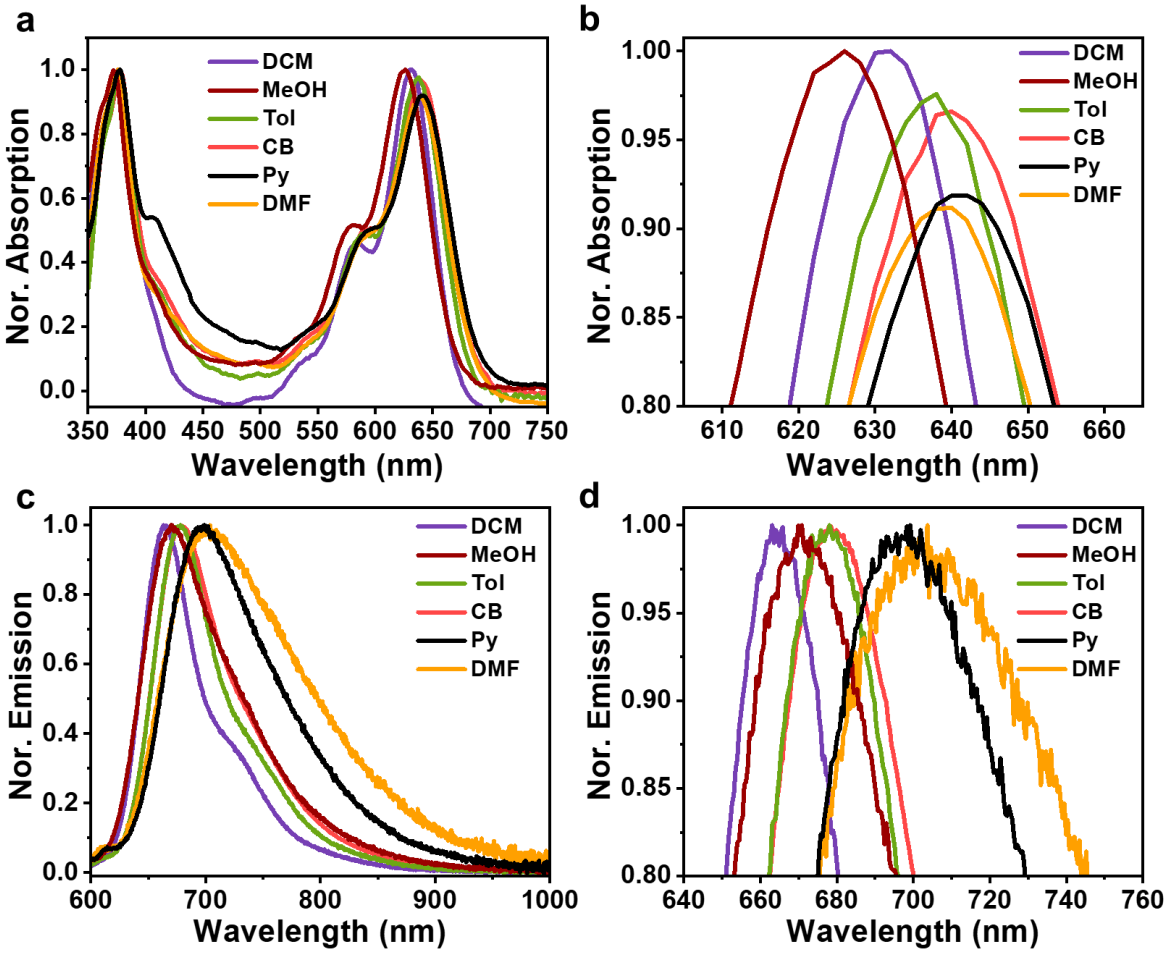

Figure S11. Normalized (a) UV-vis absorption and (c) emission spectra of DBOV–PZP **3** (2.5×10^{-6} M), as well as the corresponding enlarged normalized (b) absorption and (d) emission spectra in different argon-filled organic solvents.

5. Summarized Photophysical Parameters of DBOV–PZP 3

Table S1. Summarized photophysical parameters of DBOV–PZP **3** (2.5×10^{-6} M) in different argon-filled organic solvents.

	Tol	CB	DCM	MeOH	Py	DMF
Polarity index*	2.4	2.7	3.1	5.1	5.3	6.4
$\lambda_{max.\ abs.}$ (nm)	638	640	632	626	642	640
$\lambda_{max.\ em.}$ (nm)	678	680	663	671	699	703
Stokes shift (nm)	40	40	31	45	57	63
PLQY	0.77	0.66	0.63	0.40	0.52	0.26
Lifetime (ns)	5.9	5.2	6.2	5.0	4.8	3.4

*The polarity indices of solvents as previously reported in the literature.[4]

6. Time-Resolved Emission Spectra and Decay Profiles, as well as the Measurements of PLQY and Excitation Emission Matrix

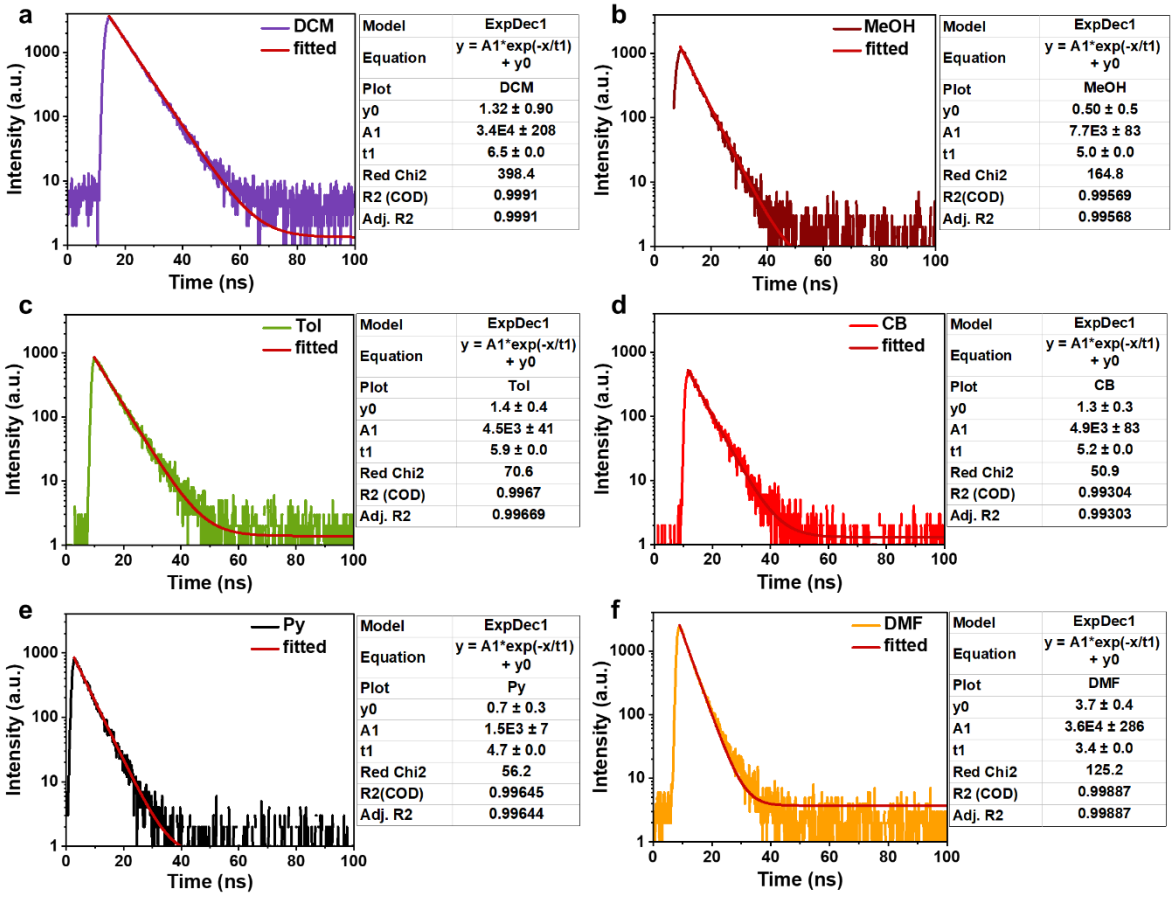

Figure S12. Emission decay profiles of DBOV–PZP **3** (2.5×10^{-6} M) at room temperature in argon-filled (a) DCM, (b) MeOH, (c) Tol, (d) CB, (e) Py, (f) DMF, respectively. Samples were excited at 380 nm and the emission intensity was integrated at the range of 585 – 845 nm.

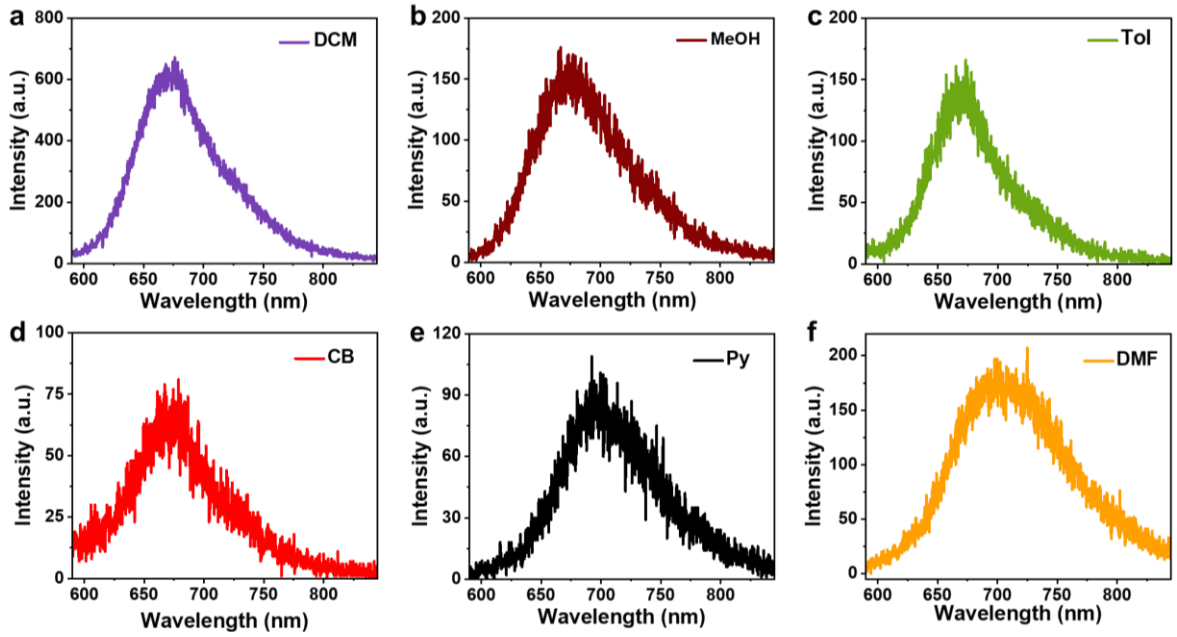

Figure S13. Time-resolved emission spectra of DBOV–PZP **3** (2.5×10^{-6} M) at room temperature in argon-filled (a) DCM, (b) MeOH, (c) Tol, (d) CB, (e) Py, (f) DMF, respectively. The samples were excited at 380 nm and the emission intensity was integrated at the range of 585 – 845 nm for 0 – 50 ns timescale.

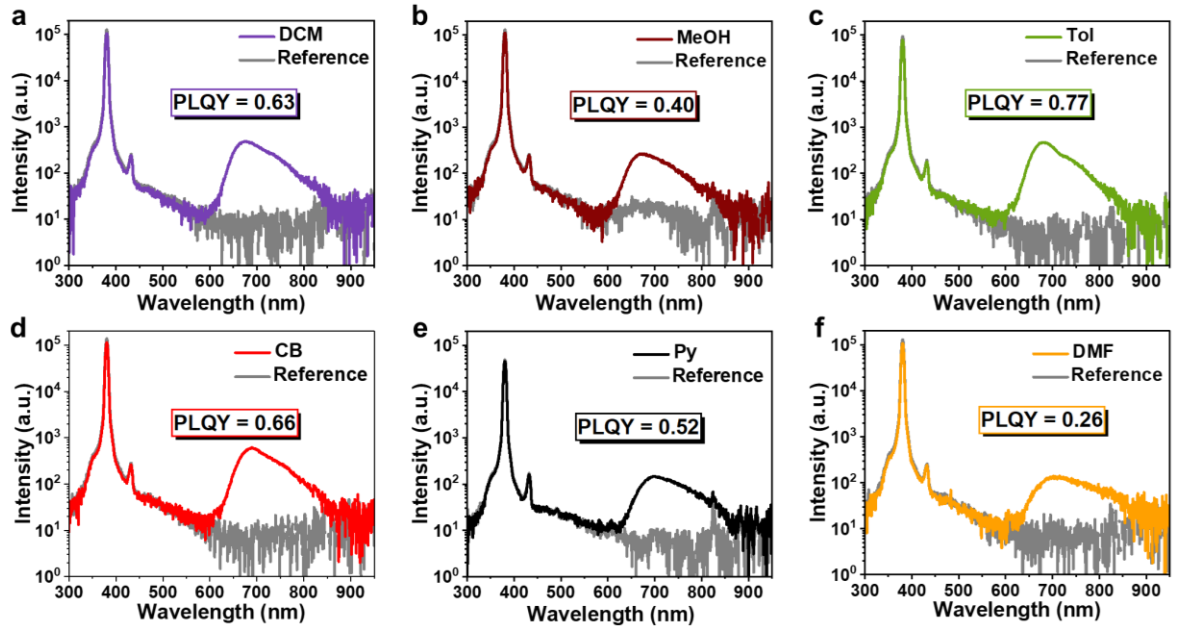

Figure S14. Emission spectra for PLQY measurements of DBOV–PZP **3** (2.5×10^{-6} M) at room temperature in argon-filled (a) DCM, (b) MeOH, (c) Tol, (d) CB, (e) Py, (f) DMF, respectively. The 380 nm wavelength was used for excitation and integration was made for a range of 580 – 940 nm for all samples.

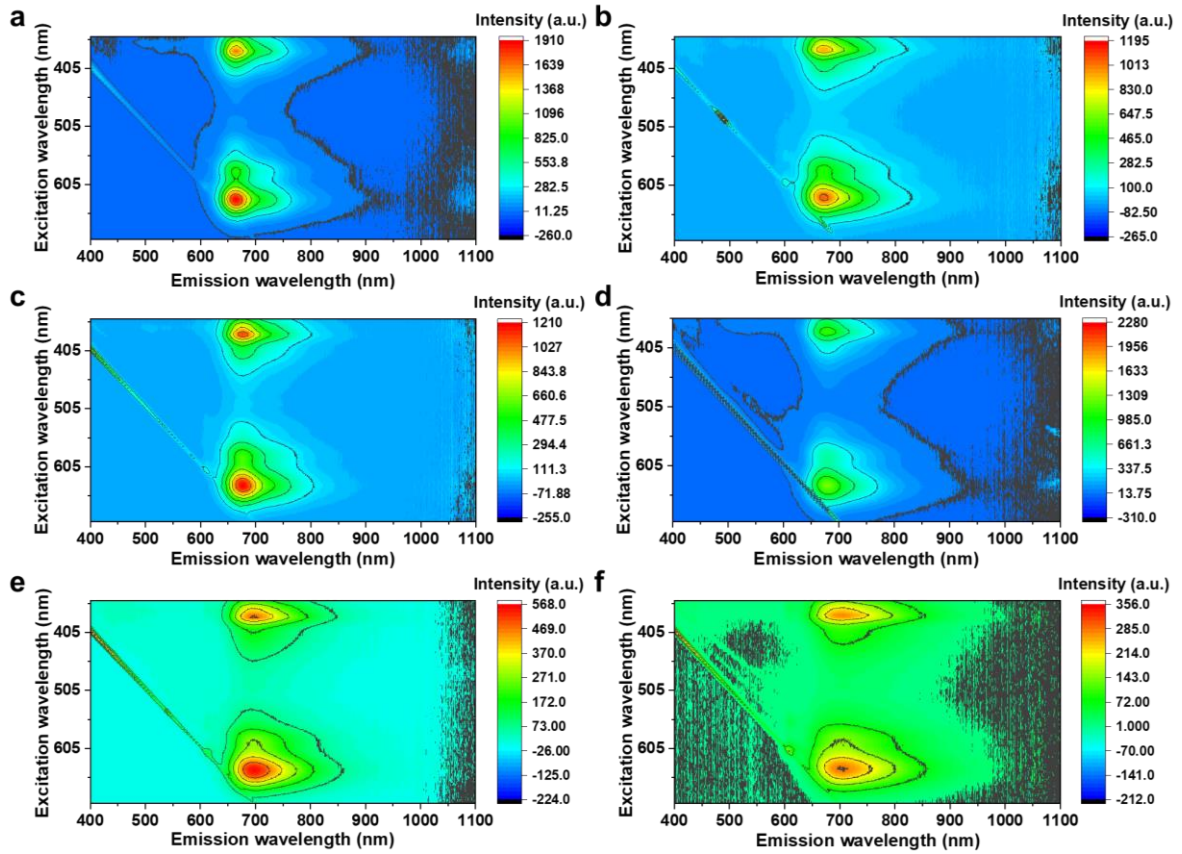

Figure S15. Excitation emission matrix of DBOV–PZP **3** (2.5×10^{-6} M) at room temperature in argon-filled (a) DCM, (b) MeOH, (c) Tol, (d) CB, (e) Py, (f) DMF, respectively.

7. Changes in the Optical Spectra of DBOV–PZP 3 upon the Addition of Acid and Base

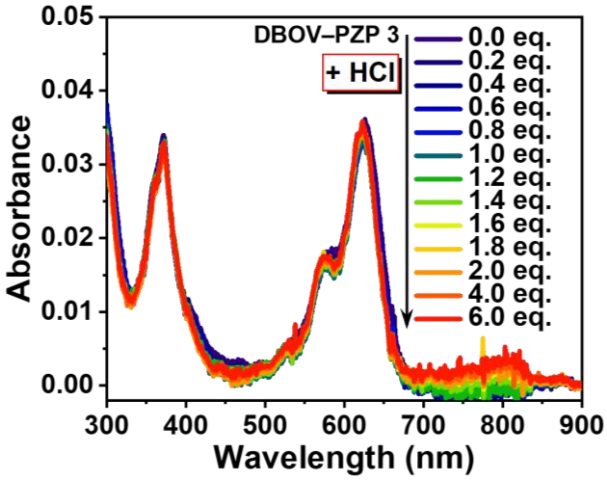

Figure S16. Changes in the UV-vis absorption spectra of DBOV–PZP **3** (2.5×10^{-6} M) in menthol upon titration with HCl.

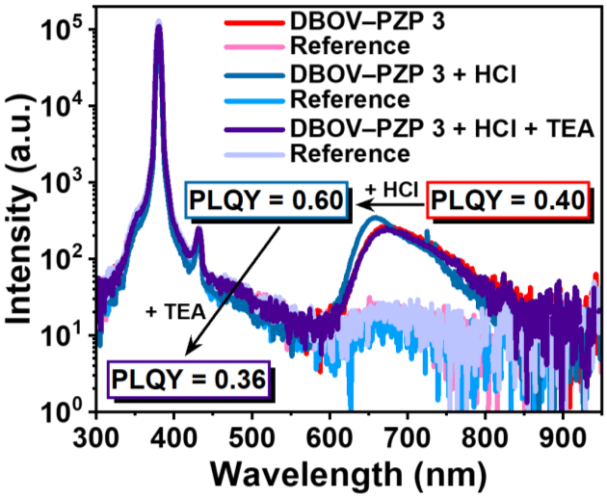

Figure S17. Changes in the emission spectra for PLQY measurements of DBOV–PZP **3** (2.5×10^{-6} M) at room temperature in argon-filled methanol, after the addition of 6 eq. of HCl, followed by neutralizing the mixture with 12 eq. of TEA.

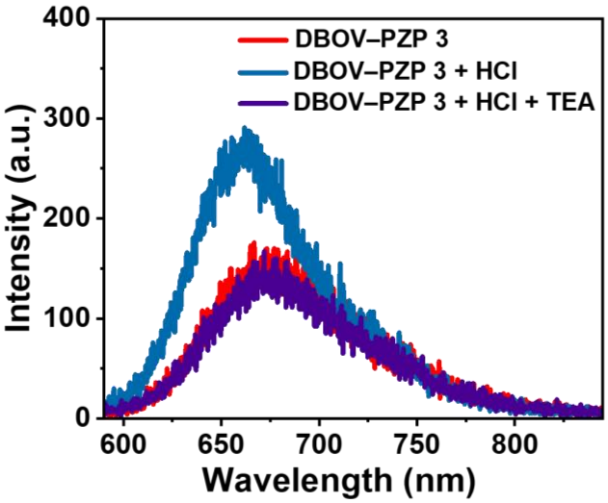

Figure S18. Changes in the time-resolved emission spectra of DBOV–PZP **3** (2.5×10^{-6} M) at room temperature in argon-filled methanol, after the addition of 6 eq. of HCl, followed by neutralizing the mixture with 12 eq. of TEA. The sample was excited at 380 nm and the emission intensity was integrated at the range of 585 – 845 nm for 0 – 50 ns timescale.

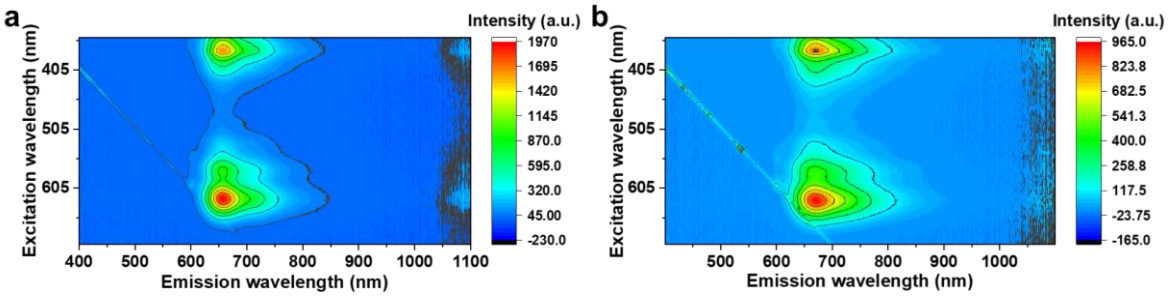

Figure S19. Changes in the excitation emission matrix of DBOV–PZP **3** (2.5×10^{-6} M) at room temperature in argon-filled methanol (a) after the addition of 6 eq. of HCl, (b) followed by neutralizing the mixture with 12 eq. of TEA.

8. Changes in the Differential Transmission Spectra of DBOV–PZP 3 upon the Addition of Acid

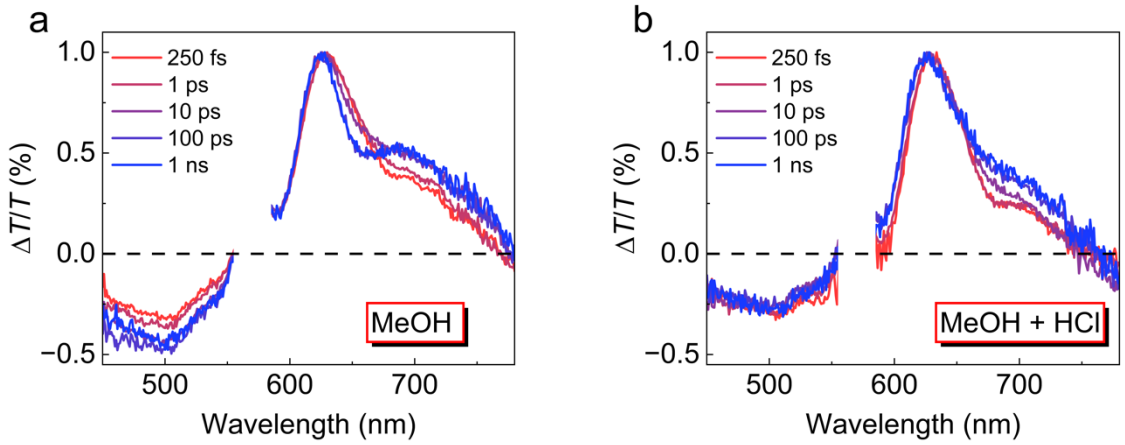

Figure S20. Differential transmission ($\Delta T/T$) spectra normalized to the maximum at various time delays between pump and probe for DBOV–PZP **3** in (a) methanol (MeOH; 1.9×10^{-4} M) and (b) MeOH after adding excess HCl. The sample was pump at λ_{pump} = 570 nm with pump power P_{pump} = 200 mW cm^{-2} (rr = 1 kHz; Δt_{pump} = 70 fs).

9. Changes in the Blinking Properties of DBOV–PZP 3 upon the Addition of Acid

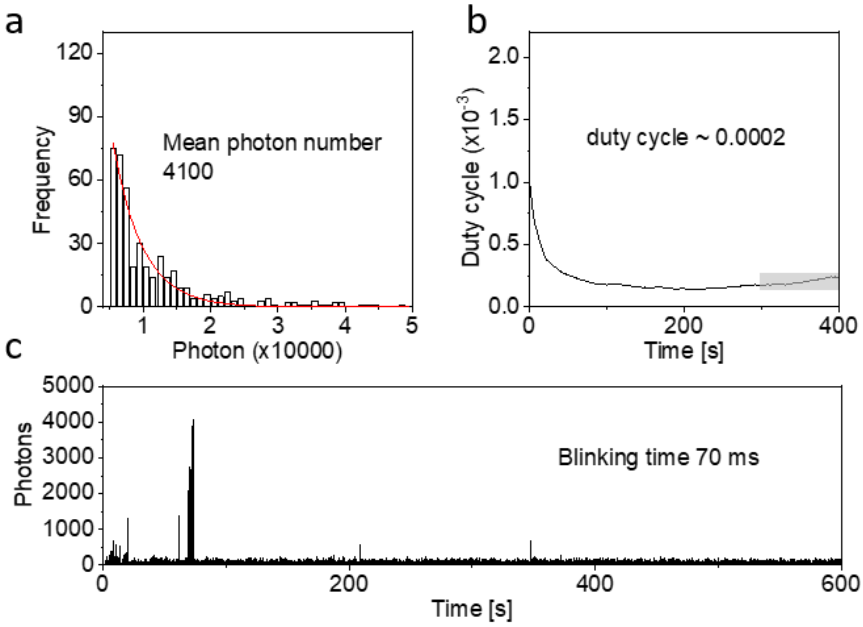

Figure S21. Blinking properties of DBOV–PZP **3** in a single molecule level measured in air. (a) Histogram of detected photons per switching event and single-exponential fit. Mean photon numbers were determined by the exponential fit. (b) On-off duty cycle calculated from single-molecule fluorescence time traces. The equilibrium duty cycle was calculated within the time window 300–400 s (gray box). (c) Representative single-molecule fluorescence time trace.

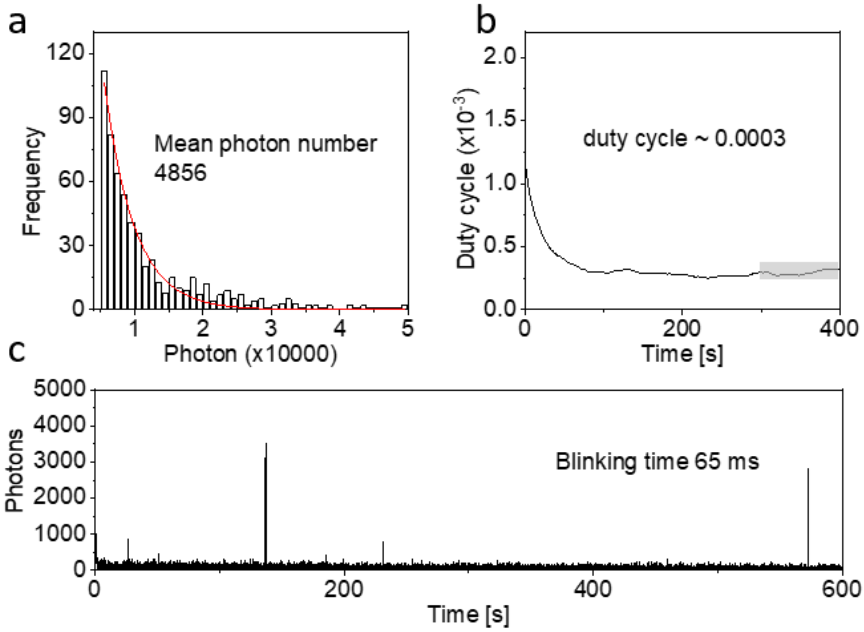

Figure S22. Blinking properties of DBOV–PZP **3** in a single molecule level measured after the addition of ~4 eq. of HCl. (a) Histogram of detected photons per switching event and single-exponential fit. Mean photon numbers were determined by the exponential fit. (b) On-off duty cycle calculated from single- molecule fluorescence time traces. The equilibrium duty cycle was calculated within the time window 300–400 s (gray box). (c) Representative single-molecule fluorescence time trace.

10. Single-molecule localization microscopy (SMLM) imaging using DBOV–PZP 3

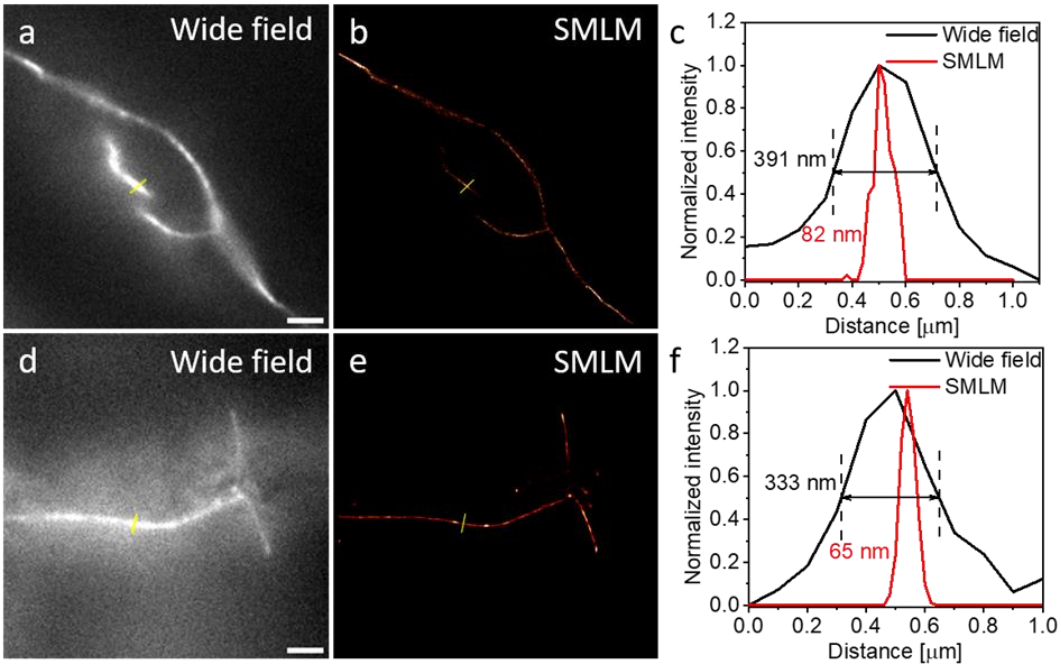

Figure S23. Fluorescence imaging of nanoscale crevices in a glass substrate using DBOV–PZP **3**, measured in air (a-c) and after the addition of ~4 eq. of HCl (d-f). The sample was prepared by depositing 10 µL of a 0.1 µM solution of DBOV–PZP **3** in dimethylformamide, with or without the addition of ~4 eq. of HCl, onto a cleaned, gridded glass coverslip. (a,d) show wide-field images, while (b,e) present the corresponding super-resolution SMLM images. Intensity profiles (c,f) of the wide-field and super-resolution SMLM images are indicated by the yellow lines in (a,b) and (d,e), respectively. Scale bar: 2 µm. A localization precision of 24 nm for DBOV–PZP **3** in acidic conditions and 25 nm in neutral conditions was achieved. The localization precision of SMLM inversely depends on the square root of detected photons per blinking event. However, factors like background signals limit this precision, especially when the detected photon number exceeds 2000. Consequently, increasing the photon count from 4100 (under neutral conditions) to 4856 (under acidic conditions) has little impact on improving localization precision.

11. Reference

1 Q. Chen, D. Wang, M. Baumgarten, D. Schollmeyer, K. Müllen and A. Narita, *Chem–Asian J.*, 2019, **14**, 1703-1707.

2 C. Manzoni and G. Cerullo, *J. Opt.*, 2016, **18**, 103501.

3 Q. Yang, E. Hosseini, P. Yao, S. Pütz, M. Gelléri, M. Bonn, S. H. Parekh and X. Liu, *J. Phys. Chem. Lett.*, 2024, **15**, 7591-7596.

4 L. R. Snyder, *J. Chromatogr. Sci.*, 1978, **16**, 223-234.